

**$(\Omega\Omega)_{0+}$ dibaryon productions in central Au+Au collisions
at RHIC energy $\sqrt{s_{NN}} = 130\text{GeV}$**

X.-M. Xu

Nuclear Physics Division, Shanghai Institute of Nuclear Research
Chinese Academy of Sciences, P.O.Box 800204, Shanghai 201800, China

P. Wang, Y. W. Yu

Institute of High Energy Physics,
Chinese Academy of Sciences, Beijing 100039, China

Abstract

Based on the measured transverse mass spectra of π^- , K^- and \bar{p} at the RHIC energy $\sqrt{s_{NN}} = 130\text{GeV}$, di-omega productions from baryon-baryon reactions in hadronic matter are studied. Results about the $(\Omega\Omega)_{0+}$ total number per event show that the deeply bound state $(\Omega\Omega)_{0+}$ can be observed at RHIC energies.

PACS codes: 14.20.Pt, 25.75.-q, 25.75.Dw,

Keywords: dibaryon, hadronic matter

1. Introduction

Data measured at RHIC experiments have revealed intriguing new features in ultrarelativistic nuclear collisions [1]. Various theoretical models have undergone challenges from the experimental data and turn out to be adjusted. The unexpected large values of the elliptic flow signal v_2 can be accounted for by hydrodynamic calculations [2] indicating perhaps complete early-time thermalization in central Au+Au collisions at $\sqrt{s_{NN}} = 130\text{GeV}$ per nucleon pair. This stresses the collective flow strongly affects hadrons in the hadronic matter produced at the center-of-mass energy. Therefore, any further predictions relying on the hadronic matter must involve available hydrodynamic behaviors.

One of the interesting topics in hadronic physics is the search for dibaryon bound states. Since dibaryon is a kind of new matter, it can provide a good place to examine the short-range quark-gluon behaviour of QCD theory and also would open a new area for studying many new physical phenomena we have not known before. Even though the H dibaryon predicted by Jaffe [3] has not been confirmed in hadron-hadron collision experiments, recently, the search is extended to Au+Au collisions in the AGS Experiment 896 [4]. Dibaryons involving Δ and nucleon were predicted in an adiabatic method [5]. Productions of short-lived dibaryons with strangeness, for instance, Σ^+p , Ξ^0p , $\Xi^0\Lambda$, $\Xi^0\Xi^-$, have been calculated for Au+Au collisions at $\sqrt{s_{NN}} = 200\text{GeV}$ and may be identified as peaks in the invariant mass spectra of final two baryons yielded from dibaryon decays [6]. Our present work is based on a dynamical investigation on dibaryon structure made in the framework of chiral $SU(3)$ model [7-9], in which the coupling between chiral fields and quarks is considered to describe the non-perturbative QCD effect, and therefore the huge data of nucleon-nucleon scattering phase shifts and hyperon-nucleon cross sections can be reproduced correctly. This investigation provided the di-omega $(\Omega\Omega)_{0+}$ as the most interesting structure [8]. It is deeply bound with the binding energy about 100MeV and its mean life time is in order of 10^{-10} second because it can only undergo through weak decay. This charged dibaryon could be easily identified in experiments carrying on ultrarelativistic nucleus-nucleus collisions[8].

In order to find the deeply bound state $(\Omega\Omega)_{0+}$ in RHIC experiments, we calculate its yield per event in central Au+Au collisions at $\sqrt{s_{NN}} = 130\text{GeV}$. As we will see in the following, the hydrodynamic equation with transverse flow is used and measured data constitute inputs in all calculations to make results as reliable as possible. Cross sections for $(\Omega\Omega)_{0+}$ yields in baryon-baryon scatterings are taken into account.

2. Hadron distributions

The hadron spectra measured in RHIC experiments allow us to analyse hadron distributions evolving with time via the Cooper-Frye formula [10], hydrodynamic equation and baryon number conservation. Assume hadron distributions are in the Boltzmann form

$$f(\lambda, p, T) = g\lambda(\tau, \eta, r)e^{-p \cdot u/T} \quad (1)$$

where g , λ , p and T are the degeneracy factor, fugacity, four-momentum and temperature, respectively. The u is the four-velocity of fluid flow given by the cylindrical polar

coordinates r , ϕ and z [11,12]. The fugacity λ depends on the proper time τ , space-time rapidity η and r . The momentum distribution of particle given by means of the Cooper-Frye formula at freeze-out time τ_{fo} is

$$\frac{d^2 N(\tau_{fo})}{m_{\perp} dm_{\perp} dy} = \frac{g\tau_{fo}}{(2\pi)^2} \int_0^{R(\tau_{fo})} dr \int_{\eta_{\min}}^{\eta_{\max}} d\eta \int_0^{2\pi} d\phi r \lambda(\tau, \eta, r) m_{\perp} \cosh(y - \eta) e^{-[m_{\perp} \cosh(y - \eta) - p_{\perp} v_r \cos \phi]/T \sqrt{1 - v_r^2}} \quad (2)$$

where N , y , p_{\perp} , m_{\perp} and v_r are respectively the number, rapidity, transverse momentum, transverse mass of hadron and transverse velocity of fluid flow. The $R(\tau_{fo})$ is the transverse radius of hadronic matter at freeze-out. The space-time rapidity spans from a minimum η_{\min} to a maximum η_{\max} . Any measured spectra of hadrons allow one to determine fugacities and transverse velocity at freeze-out. To gain the velocity profile at any proper time τ , the hydrodynamic equation is used,

$$\partial_{\mu} T^{\mu\nu} = 0 \quad (3)$$

where the energy-momentum tensor is

$$T^{\mu\nu} = (\epsilon + P)u^{\mu}u^{\nu} + P g^{\mu\nu} \quad (4)$$

The ϵ and P are energy density and pressure, respectively. Because the dominant ingredient of hadronic matter is assumed to be pions, the equation of state is $\epsilon = 3P$. With the hydrodynamic equation for a boost-invariant longitudinal expansion along the z axis and a cylindrically symmetric transverse expansion [11], the transverse velocity $v_r(\tau, r)$ at any time prior to freeze-out is obtained.

The dependence of hadron fugacity on time is obtained by the number conservation

$$\partial_{\mu}(n u^{\mu}) = 0 \quad (5)$$

which is followed by [13]

$$\partial_t \lambda + v_r \partial_r \lambda + \frac{\lambda}{\gamma T^3} \partial_t (\gamma T^3) + \frac{\lambda v_r}{\gamma T^3} \partial_r (\gamma T^3) + \lambda \partial_r v_r + \lambda \left(\frac{v_r}{r} + \frac{1}{t} \right) = 0 \quad (6)$$

where $\gamma = 1/\sqrt{1 - v_r^2}$.

The equation for fugacity has the divergent term $\lambda v_r/r$ as $r \rightarrow 0$, which causes difficulty in solving numerically the equation and leads to nonphysical solutions. There are four cases on curing this divergence:

- (1) $v_r \sim r^n$ as $r \rightarrow 0$ with $n \geq 1$;
- (2) $\lambda \sim r^m$ as $r \rightarrow 0$ with $m \geq 1$;
- (3) $v_r \sim r^n$ and $\lambda \sim r^m$ with $n < 1$ and $m < 1$ but $n + m < 1$ while $r \rightarrow 0$;
- (4) The term $\frac{\lambda v_r}{\gamma T^3} \partial_r (\gamma T^3)$ cancels this term $\frac{\lambda v_r}{r}$ as $r \rightarrow 0$,

$$\frac{\lambda v_r}{\gamma T^3} \partial_r (\gamma T^3) + \frac{\lambda v_r}{r} = 0 \quad (7)$$

which has the analytic solution

$$T = \left(\frac{C_1}{\gamma r} \right)^{\frac{1}{3}} \quad (8)$$

The constant C_1 is positive and in general depends on time. This solution becomes unphysical if it is singular as $r \rightarrow 0$. To avoid this, mandatorily force $\gamma r = C_2$ with C_2 being nonzero and positive. The consequence is

$$v_r = \sqrt{1 - \left(\frac{r}{C_2}\right)^2} \quad (9)$$

Then the condition $C_2 > r$ is required to give real transverse velocity.

Before doing any calculations, we assume the hadronic matter freezing out at $\tau_{fo} = 10\text{fm}/c$ has a transverse radius $R(\tau_{fo}) = 10\text{fm}$. The fugacity takes a form independent of η and has the same dependence on r for all sorts of hadrons except for different normalizations to fit rapidity densities. Given some trial functions for fugacities and velocities, the transverse mass spectra of π^- , K^- and \bar{p} at mid-rapidity in central Au+Au collisions at $\sqrt{s_{NN}} = 130\text{GeV}$ in Ref. [14] are reproduced. We find the following parametrizations showing r -dependences of fugacities and transverse velocity profiles at freeze-out

$$\lambda_{fo} \propto r^4 e^{-0.7r}, \quad v_r = \left(\frac{9.65 + r}{20.3}\right)^3 \quad (10)$$

in the case (2) and

$$\lambda_{fo} \propto \frac{e^{0.2r}}{r^{0.3}}, \quad v_r = \sqrt{1 - \left(\frac{r}{10.1}\right)^2} \quad (11)$$

in the case (4). Inserting the fugacities and transverse velocities into Eq. (1), we obtain hadron distributions as $r \rightarrow 0$: $f \rightarrow 0$. Evolve the hydrodynamic equation and the fugacity equation (6) back to a previous time from the freeze-out hypersurface, we still have $f \rightarrow 0$ as $r \rightarrow 0$ while the transverse velocity is kept as $r \rightarrow 0$ as nonzero for the case (2) and the analytic function in Eq. (9) remains with a τ -dependence of C_2 for the case (4). Such f conflicts with the finite amplitude of a real hadron distribution as $r \rightarrow 0$. The cases (2) and (4) are therefore given up. Undoubtedly, nonzero hadron distributions beginning with the formation of hadronic matter may be found by seeking for a specific numerical method. But we do not consider here this task since we have no intention of finding all solutions of the hydrodynamic equation and the fugacity equation in coordinate space and all hadron distributions via Eq. (2) on the freeze-out hypersurface. Parametrizations for the fugacity and transverse velocity with the small r behavior described in the case (3) are not found.

In the case (1) the fugacity and transverse velocity are not unique. The first set is

$$\lambda_{fo} \propto \begin{cases} 1, & r < 7.5 \\ e^{-(r-7.5)^2}, & r \geq 7.5 \end{cases} \quad v_r = \frac{r}{10.4} \quad (12)$$

The v_r depends linearly on r like Ref. [15]. The second and third sets of parametrizations are

$$\lambda_{fo} \propto \begin{cases} 1, & r < \pi \\ e^{-(r-\pi)}, & r \geq \pi \end{cases} \quad v_r = \tanh \frac{r}{4.8} \quad (13)$$

$$\lambda_{fo} \propto \begin{cases} 1, & r < \frac{\pi}{2} \\ e^{-(2r-\pi)}, & r \geq \frac{\pi}{2} \end{cases} \quad v_r = \tanh \frac{r}{2.4} \quad (14)$$

In fact, the third set is obtained from the second set by making the replacement $r \rightarrow 2r$. For $r > R(\tau_{fo})$ the fugacity in the exponential form gives very small value and has negligible contribution to the integration over r . Then $\int_0^{R(\tau_{fo})} dr = \int_0^{2R(\tau_{fo})} dr$ is a very good approximation and the two sets give the same dependence of $d^2N/m_\perp dm_\perp dy$ on the transverse mass upon normalization. Actually, the substitution $r \rightarrow ar$ with $a > 1$ leads to a class of fugacities and transverse velocities

$$\lambda_{fo} \propto \begin{cases} 1, & r < \frac{\pi}{a} \\ e^{-(ar-\pi)}, & r \geq \frac{\pi}{a} \end{cases} \quad v_r = \tanh \frac{ar}{4.8} \quad (15)$$

which fits well the measured data of $d^2N/m_\perp dm_\perp dy$ versus m_\perp for π^- , K^- and \bar{p} . Since the three curves in Fig. 1 of Ref. [14] are plotted in arbitrary units, the rapidity density $\frac{dN}{dy} = \int_m^\infty m_\perp dm_\perp \frac{d^2N}{m_\perp dm_\perp dy}$ is fitted to that generated in HIJING/B \bar{B} [16] for p , \bar{p} , n and \bar{n} , respectively. In this way the magnitude of fugacity is completely fixed and the minimum and maximum of η are individually equal to -4 and 4 for nucleon, -2.8 and 2.8 for antinucleon. Meanwhile, a common freeze-out temperature $T = 0.1\text{GeV}$ is obtained for π^- , K^- and \bar{p} as extracted in Ref. [14].

Define an average velocity

$$\bar{v}_r = \frac{\int_0^{R(\tau_{fo})} dr v_r}{R(\tau_{fo})} \quad (16)$$

The three sets of transverse velocity profiles in Eqs. (12)-(14) give $\bar{v}_r \approx 0.48c, 0.67c, 0.83c$, respectively.

As already mentioned the measured data at RHIC energy might not well be reproduced in some theoretical models. The produced Ω spectra is unknown. Even the knowledge of Ω^- spectra measured in CERN-SPS experiments is very limited. To have a good sense on the Ω^- spectra, we utilize the experimental data on the ratio of antiproton yield at RHIC to that at CERN-SPS. Since both the antiproton and Ω^- at mid-rapidity can be created from junction and pomeron [16,17], we assume the ratio of Ω^- yield at RHIC to that at CERN-SPS is the same as the ratio for antiproton. For rapidity densities of Ω^- and antiproton,

$$\frac{dN_{\Omega^-,RHIC}}{dy} / \frac{dN_{\Omega^-,SPS}}{dy} = \frac{dN_{\bar{p},RHIC}}{dy} / \frac{dN_{\bar{p},SPS}}{dy} \quad (17)$$

It follows that

$$\frac{dN_{\Omega^-,RHIC}}{dy} = C \frac{dN_{\bar{p},RHIC}}{dy} \quad (18)$$

where

$$C = \frac{dN_{\Omega^-,SPS}}{dy} / \frac{dN_{\bar{p},SPS}}{dy} \quad (19)$$

is taken as a constant and determined at mid-rapidity by

$$C = \int_{-0.5}^{0.5} dy \frac{dN_{\Omega^-,SPS}}{dy} / \int_{-0.5}^{0.5} dy \frac{dN_{\bar{p},SPS}}{dy} \quad (20)$$

If the numerator is estimated from the values measured by WA97 Collaboration [18] and the denominator by NA49 Collaboration [19], C is about equal to 0.01.

3. Number of $(N\Omega)_{2+}$

The chiral $SU(3)$ quark model with the scalar nonet fields and pseudoscalar nonet fields has been presented to study $(\Omega\Omega)_{0+}$ productions in baryon-baryon scatterings [20,21]. To create such a deeply bound state, the electromagnetic process

$$\Omega + \Omega \rightarrow (\Omega\Omega)_{0+} + \gamma \quad (21)$$

and the mesonic process

$$\Omega + \Omega \rightarrow (\Omega\Omega)_{0+} + \eta \quad (22)$$

are considered first. Since the state $(\Omega\Omega)_{0+}$ is directly produced from two Ω baryons, the two reactions are called direct production processes. In order to understand physics well, the cross sections in Ref. [20] are replotted as functions of the center-of-mass energy of the two incoming omegas, \sqrt{s} , in Fig. 1.

The chiral $SU(3)$ quark model shows a weakly bound state $(N\Omega)_{2+}$ composed of a nucleon and an omega. The $(N\Omega)_{2+}$ dibaryon with spin 2 and positive parity can be formed through the electromagnetic process

$$\Omega + N \rightarrow (N\Omega)_{2+} + \gamma \quad (23)$$

and the mesonic process

$$\Omega + N \rightarrow (N\Omega)_{2+} + \pi \quad (24)$$

This $(N\Omega)_{2+}$ state enhances the yield of $(\Omega\Omega)_{0+}$ by three-quark exchange processes during its collisions with Ω baryons

$$\Omega + (N\Omega)_{2+} \rightarrow (\Omega\Omega)_{0+} + N \quad (25)$$

Such $(\Omega\Omega)_{0+}$ dibaryon is yielded from the collision of Ω with nucleon and the accompanying product $(N\Omega)_{2+}$. The reactions are called indirect production processes. For present calculations it is better to redraw the cross sections in Ref. [21] as functions of the center-of-mass energy of omega and nucleon in Fig. 2 and of omega and $(N\Omega)_{2+}$ in Fig. 3.

The number of $(N\Omega)_{2+}$ contained in hadronic matter at a proper time τ is

$$N_{(N\Omega)_{2+}} = \int d^4x \int \frac{d^3p_\Omega}{(2\pi)^3} f_\Omega(\lambda_\Omega, p_\Omega, T) \int \frac{d^3p_N}{(2\pi)^3} f_N(\lambda_N, p_N, T) v_{rel} \sigma_{N\Omega}(\sqrt{s}) \quad (26)$$

which has the volume $\int d^4x = \int_0^{2\pi} d\phi \int_{\tau_f}^\tau d\tau \int_0^{R(\tau)} dr r \int_{\eta_{\min}}^{\eta_{\max}} d\eta$ and where v_{rel} is the relative velocity of two scattering particles and $\sigma_{N\Omega}$ is the sum of cross sections for the reactions (23) and (24). The number of dibaryon $(N\Omega)_{2+}$ is calculated for a central Au+Au collision at $\sqrt{s_{NN}} = 130\text{GeV}$. Results are plotted in Fig. 4. We take the hypothesis that $(N\Omega)_{2+}$ thermalizes immediately in hadronic matter once it is created. Then the momentum distribution of $(N\Omega)_{2+}$ satisfies the Boltzmann form and the corresponding fugacity is determined by

$$N_{(N\Omega)_{2+}}(\tau) = \frac{g\tau}{(2\pi)^2} \int_0^{R(\tau)} dr \int_{\eta_{\min}}^{\eta_{\max}} d\eta \int_0^{2\pi} d\phi \int_{m_{N\Omega}}^\infty dm_\perp \int_{-\infty}^{+\infty} dy r \lambda_{N\Omega}(\tau, \eta, r) m_\perp^2 \cosh(y - \eta) e^{-[m_\perp \cosh(y - \eta) - p_\perp v_r \cos \phi]/T \sqrt{1 - v_r^2}} \quad (27)$$

where $m_{N\Omega}$ is the dibaryon mass. The dibaryon fugacity $\lambda_{N\Omega}$ takes the same r -dependence as a baryon except for normalization.

4. Di-omega productions per event

While the momentum distributions of Ω and $(N\Omega)_{2+}$ are known, the di-omega yield per event is calculated via the formula

$$N = \int d^4x \int \frac{d^3p_1}{(2\pi)^3} f_1(\lambda_1, p_1, T) \int \frac{d^3p_2}{(2\pi)^3} f_2(\lambda_2, p_2, T) v_{rel} \sigma_{\Omega\Omega}(\sqrt{s}) \quad (28)$$

where $\int d^4x = \int_0^{2\pi} d\phi \int_{\tau_f^o}^{\tau_f} d\tau \int_0^{R(\tau)} dr r \int_{\eta_{\min}}^{\eta_{\max}} d\eta$ with $\tau_f = 1.5\text{fm}/c$ corresponding to the temperature $T \approx 0.19\text{GeV}$. At the moment of forming hadronic matter, the interacting glod-gold system has already expanded. Presumably, the $R(\tau)$ grows linearly with the proper time from $R(\tau_f) = 7\text{fm}$ to $R(\tau_{fo}) = 10\text{fm}$. The $\sigma_{\Omega\Omega}$ include cross sections for the reactions (21), (22) and (25).

Given a fugacity and transverse flow velocity, number of dibaryon $(\Omega\Omega)_{0+}$ yielded in a central Au+Au collision at $\sqrt{s_{NN}} = 130\text{GeV}$ is listed in Table 1. N_1 , N_2 and N_5 are individually the number of $(\Omega\Omega)_{0+}$ created through the reactions $\Omega + \Omega \rightarrow (\Omega\Omega)_{0+} + \gamma$, $\Omega + \Omega \rightarrow (\Omega\Omega)_{0+} + \eta$ and $\Omega + (N\Omega)_{2+} \rightarrow (\Omega\Omega)_{0+} + N$. The total number obtained in the work is

$$N_{tot} = N_1 + N_2 + N_5 \quad (29)$$

where N_1 , N_2 and N_5 are calculated with the use of Eq. (28).

5. Discussions and conclusions

We have shown that different hadron distributions at freeze-out lead to different $(\Omega\Omega)_{0+}$ numbers produced in a Au+Au collision and have obtained that π^- , K^- and \bar{p} freeze out at the same temperature $T = 0.1\text{GeV}$ while the radius of transverse extension of cylindrically symmetric hadronic matter is 10fm. If the freeze-out temperature or transverse radius changes, these distributions vary. The fugacities and transverse velocities in Eqs. (14) and (15) result from the replacement $r \rightarrow 2r$ and $r \rightarrow ar$ in the parametrization (13). However, the hydrodynamic equation and the fugacity equation (6) are not invariant under the replacement. This is one reason why the number of $(\Omega\Omega)_{0+}$ corresponding to the parametrization (13) is different from that to the other parametrization (14). Another reason is that a factor a^2 accounts for the variation of the integration $\int dr r$ under the replacement $r \rightarrow ar$.

In the indirect production processes the number of $(N\Omega)_{2+}$ depends on the freeze-out temperature, the final transverse radius and the final proper time when the hadronic matter becomes free particles. The yield of $(\Omega\Omega)_{0+}$ in the indirect production processes is actually proportional to the square of the distributions of proton and neutron. Fig. 4 exhibits very small number of $(N\Omega)_{2+}$. However, the cross sections for each of indirect production processes, especially the exothermal reaction $\Omega + (N\Omega)_{2+} \rightarrow (\Omega\Omega)_{0+} + N$ in Fig. 3, are much larger than the cross sections for the direct production processes. The amount of di-omega gained in the indirect production processes eventually exceeds that in the direct production processes. Nevertheless, this is true only near freeze-out when

the $(N\Omega)_{2+}$ number is relatively larger, and false near hadronization when the $(N\Omega)_{2+}$ number is lack.

It is shown by the three curves in Fig. 4 that the $(N\Omega)_{2+}$ dibaryon number increases rapidly during the time interval from $\tau = 1.5\text{fm}/c$ to $3\text{fm}/c$. Almost all of $(N\Omega)_{2+}$ are produced in the early time of hadronic matter and sensitive to early-time thermalization. The variation of dibaryon number with time is controlled by high baryon densities in the early time of hadronic matter and later on low baryon densities. We are also interested in calculating the dependence of $(\Omega\Omega)_{0+}$ number on the proper time with, for instance, the fugacity and transverse velocity in Eq. (12). Unlike the $(N\Omega)_{2+}$, we find that the di-omega number changes slowly with time and almost all of $(\Omega\Omega)_{0+}$ are produced in the late time of hadronic matter. Even if the $(N\Omega)_{2+}$ number increases rapidly, its density rises up not fast because the matter volume increases. Together with the reducing density of Ω^- with time, the $(\Omega\Omega)_{0+}$ is produced slowly in hadronic matter.

The reaction $\Omega + \Omega \rightarrow (\Omega\Omega)_{0+} + \eta$ has the threshold energy 3.776GeV higher than the value 3.344GeV for $\Omega + \Omega \rightarrow (\Omega\Omega)_{0+} + \gamma$. Peaks of cross sections are shown in Fig. 1 for both reactions. Thereby the Ω has larger average energy in the η yield process than in the γ yield process. This considerably reduces the $(\Omega\Omega)_{0+}$ yield from the former reaction compared to the latter by the momentum distribution of Ω . However, the ratio $N_2/N_1 \approx 2.5$ in Table 1 reverse the case. This comes out of the following factors: the reaction for η production has larger cross section and a wider peak than for γ ; higher relative velocity of two Ω s is demanded for η production; $d^3p_1 d^3p_2$ in Eq. (28) is greatly enhanced by the larger average momentum of Ω needed for η yield. Therefore, more $(\Omega\Omega)_{0+}$ dibaryons are produced in the η yield process than in the γ yield process.

We have not estimated di-omega yields in the expansion process from the moment of initial nucleus-nucleus collision to the time $\tau_f = 1.5\text{fm}/c$ when hadronic matter appears. During this period the central Au+Au collision at $\sqrt{s_{NN}} = 130\text{GeV}$ may lead to deconfined gluons and quarks in nonequilibrium, if we believe at CERN-SPS energy the Pb+Pb collisions are on the boundary of phase transition involving hadronic and partonic degrees of freedom. While the quarks and gluons hadronize at τ_f , it is possible for six strange quarks to combine into a dibaryon $(\Omega\Omega)_{0+}$ as well as six light quarks to form $(N\Omega)_{2+}$. Then the number of $(N\Omega)_{2+}$ at $\tau_f = 1.5\text{fm}/c$ is not zero and moves upwards these curves in Fig. 4.

It is unavoidable to address in-medium effect on the production of $(\Omega\Omega)_{0+}$. The mass of strange quark is reduced and the quark-quark potential is screened in hadronic matter at finite temperature. Obviously the screening decreases the binding energy of $(\Omega\Omega)_{0+}$. However, the kinetic-energy contribution increases the binding energy by the dropping mass of strange quark. We can still expect an appreciable binding energy for $(\Omega\Omega)_{0+}$ in hadronic matter with reference to the large binding energy of free $(\Omega\Omega)_{0+}$. In addition, hadronic matter modifies the relative-motion wave function of two omegas inside the dibaryon and the coupling of η to Ω in $\Omega + \Omega \rightarrow (\Omega\Omega)_{0+} + \eta$ and the coupling of π to N in $\Omega + N \rightarrow (N\Omega)_{2+} + \pi$. These result in different cross sections for the direct and indirect production processes in comparison to Figs. 1-3 and different $(\Omega\Omega)_{0+}$ number yielded relative to Table 1. Exploring in-medium effect remains in a future work.

In conclusion, we have obtained the number of dibaryon $(\Omega\Omega)_{0+}$ produced in a central Au+Au collision at $\sqrt{s_{NN}} = 130\text{GeV}$ is of the order of $10^{-9} \sim 10^{-7}$. Even if the number is very small, enough events will be accumulated to observe the yield in the coming years

of running of RHIC machine. Besides, we have shown: the mesonic processes have larger contributions than the electromagnetic processes; at freeze-out the indirect production processes have larger contributions than the direct production processes; di-omegas are mostly produced in late-time hadronic matter.

Acknowledgements

We wish to thank X. N. Wang, N. Xu and Z. Y. Zhang for useful helps. This work was supported by the National Natural Science Foundation of China, the fund of Science and Technology Committee of Shanghai and the CAS Knowledge Innovation Project No. KJCX2-SW-N02.

References

- [1] For reviews see *Proceedings of Quark Matter 2001*, SUNY, Jan. 15-20.
- [2] STAR Collaboration, K. H. Ackermann *et al.*, Phys. Rev. Lett. 86(2001)402;
P. F. Kolb, U. Heinz, P. Huovinen, K. J. Eskola, K. Tuominen, Nucl. Phys. A696(2001)197;
D. Teaney, J. Lauret, E. V. Shuryak, Nucl. Phys. A698(2002)479.
- [3] R. L. Jaffe, Phys. Rev. Lett. 38(1977)195.
- [4] E896 Collaboration, H. Caines *et al.*, Nucl. Phys. A661(1999)170c.
- [5] F. Wang, J. Ping, G. Wu, L. Teng, T. Goldman, Phys. Rev. C51(1995)3411;
T. Goldman, K. Maltman, G. J. Stephenson Jr., J. Ping, F. Wang, Mod. Phys. Lett. A13(1997)59.
- [6] J. Schaffner-Bielich, R. Mattiello, H. Sorge, Phys. Rev. Lett. 84(2000)4305.
S. D. Paganis, G. W. Hoffmann, R. L. Ray, J.-L. Tang, T. Udagawa, R. S. Longacre, Phys. Rev. C62(2000)024906.
- [7] Z. Y. Zhang, Y. W. Yu, L. R. Dai, High Energy Phys. Nucl. Phys. 20(1996)363;
Z. Y. Zhang, Y. W. Yu, P. N. Shen, L. R. Dai, A. Faessler and U. Straub, Nucl. Phys. A625(1997)59.
- [8] Y. W. Yu, Z. Y. Zhang, X. Q. Yuan, Commun. Theor. Phys. 31(1999)1;
Z. Y. Zhang, Y. W. Yu, C. R. Ching, T. H. Ho, Z. D. Lu, Phys. Rev. C61(2000)065204.
- [9] Q. B. Li, P. N. Shen, Z. Y. Zhang, Y. W. Yu, Nucl. Phys. A683(2001)487.
- [10] F. Cooper, G. Frye, Phys. Rev. D10(1974)186.
- [11] H. von Gersdorff, L. McLerran, M. Kataja, P. V. Ruuskanen, Phys. Rev. D34(1986)794.
- [12] E. Schnedermann, J. Sollfrank, U. Heinz, Phys. Rev. C48(1993)2462.
- [13] D. K. Srivastava, M. G. Mustafa, B. Müller, Phys. Rev. C56(1997)1064.
- [14] N. Xu, M. Kaneta, in *Proceedings of Quark Matter 2001*, SUNY, Jan. 15-20.
- [15] T. S. Biró, Phys. Lett. B487(2000)133.
- [16] S. E. Vance, M. Gyulassy, X.-N. Wang, Phys. Lett. B443(1998)45;
S. E. Vance, M. Gyulassy, Phys. Rev. Lett. 83(1999)1735.
- [17] D. Kharzeev, Phys. Lett. B378(1996)238.
- [18] WA97 Collaboration, E. Andersen *et al.*, Phys. Lett. B449(1999)401;
J. Phys. G25(1999)171.
- [19] NA49 Collaboration, F. Siklér *et al.*, Nucl. Phys. A661(1999)45c.
- [20] Y. W. Yu, P. Wang, Z. Y. Zhang, C. R. Ching, T. S. Ho, Commun. Theor. Phys. 35(2001)553.
- [21] Y. W. Yu, P. Wang, Z. Y. Zhang, C. R. Ching, T. S. Ho and L. Y. Chu, High Energy Phys. Nucl. Phys. (to be published).

Figure captions

Fig. 1. The left and right panels show cross sections for $\Omega + \Omega \rightarrow (\Omega\Omega)_{0+} + \gamma$ and $\Omega + \Omega \rightarrow (\Omega\Omega)_{0+} + \eta$, respectively, as functions of the center-of-mass energy of two incident omegas.

Fig. 2. Dotted, dot-dashed and solid lines in the left panel show cross sections for $\Omega + p \rightarrow (p\Omega)_{2+} + \gamma$, $\Omega + n \rightarrow (n\Omega)_{2+} + \gamma$ and their sum, respectively. The right panel shows the cross section for $\Omega + N \rightarrow (N\Omega)_{2+} + \pi$ where N includes proton and neutron.

Fig. 3. Cross section for $\Omega + (N\Omega)_{2+} \rightarrow (\Omega\Omega)_{0+} + N$ as a function of the center-of-mass energy \sqrt{s} . The N includes proton and neutron.

Fig. 4. Solid, dashed and dot-dashed lines are the numbers of $(N\Omega)_{2+}$ produced with the parametrizations for fugacities and transverse velocities in Eqs. (12)-(14), respectively.

Table 1: Number of $(\Omega\Omega)_{0+}$ produced per event with the three sets of fugacities and transverse velocities in Eqs. (12)-(14).

	Eq.(12)	Eq.(13)	Eq.(14)
N_1	9.29×10^{-10}	2.82×10^{-9}	1.13×10^{-8}
N_2	2.27×10^{-9}	7.57×10^{-9}	2.92×10^{-8}
N_5	3.43×10^{-9}	3.6×10^{-8}	5.95×10^{-7}
N_{tot}	6.63×10^{-9}	4.64×10^{-8}	6.35×10^{-7}

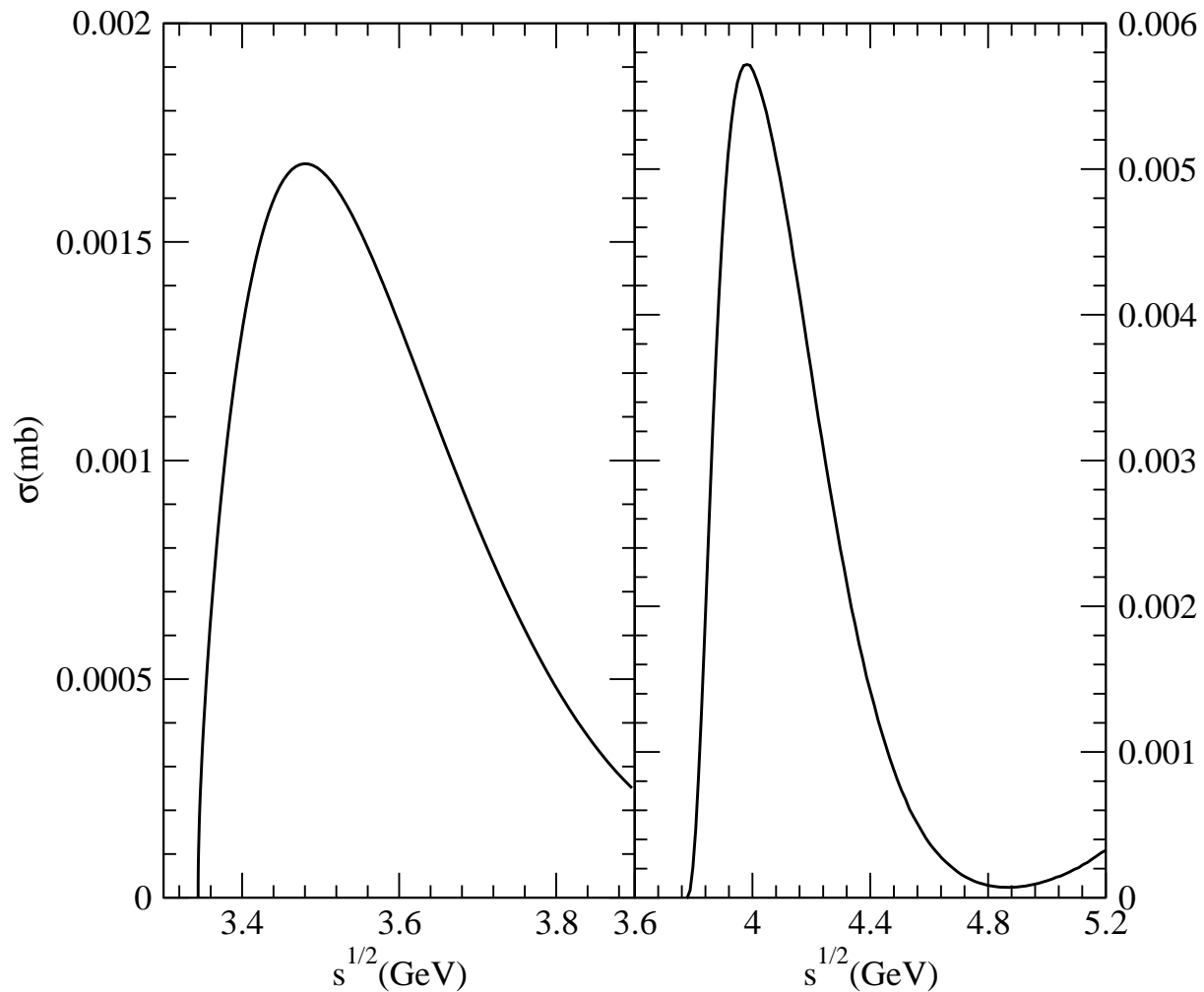


Figure 1:

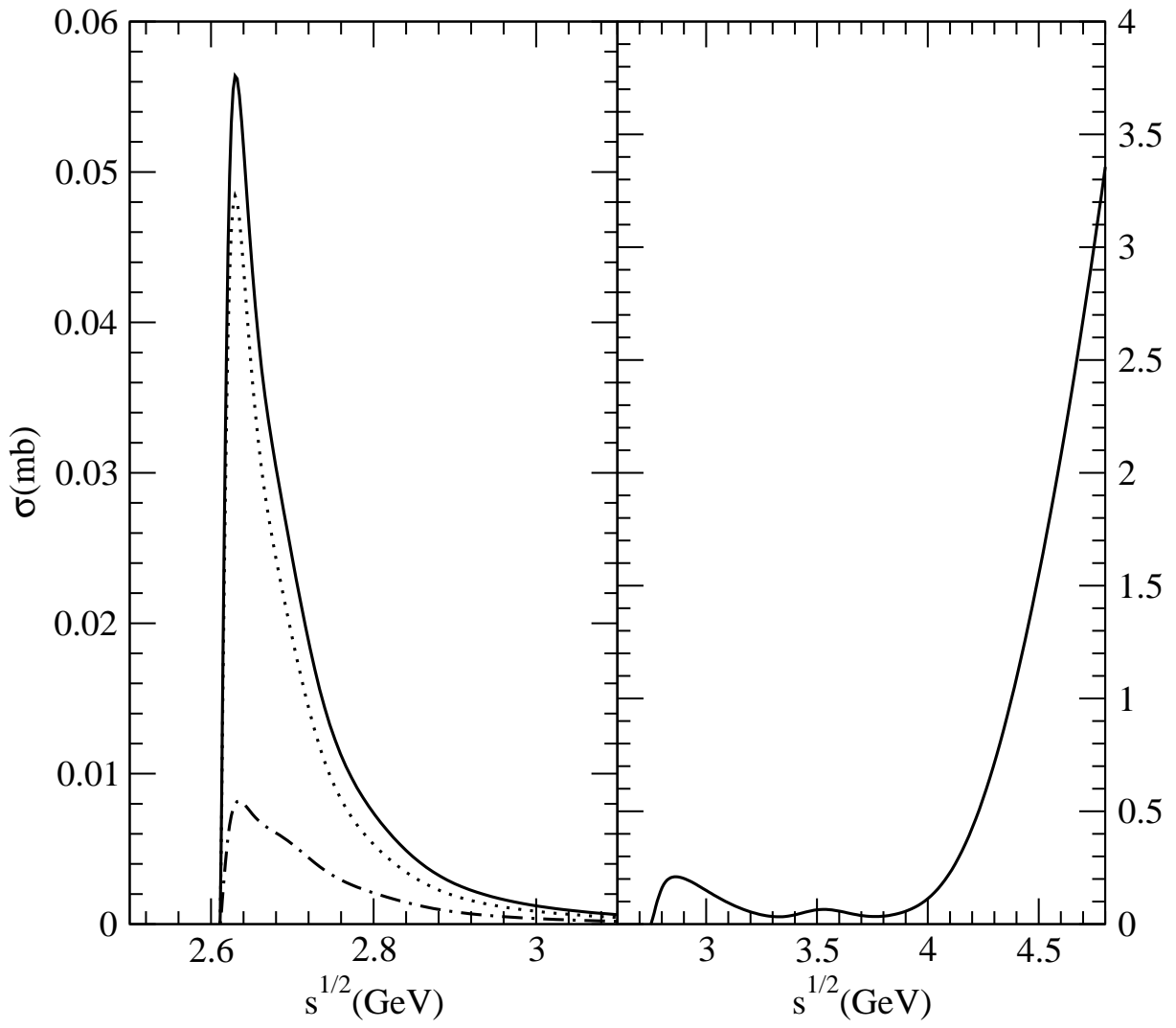


Figure 2:

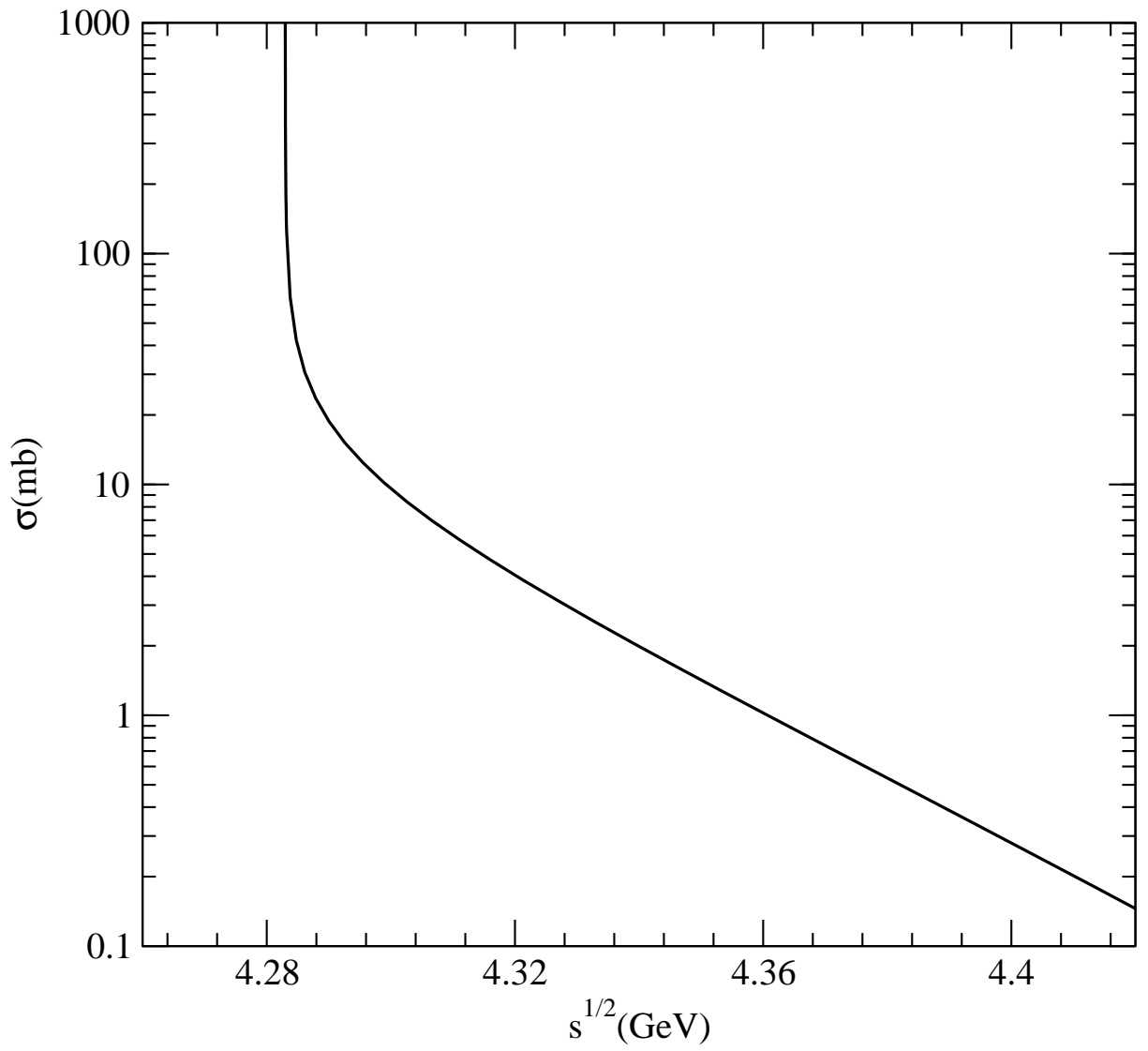


Figure 3:

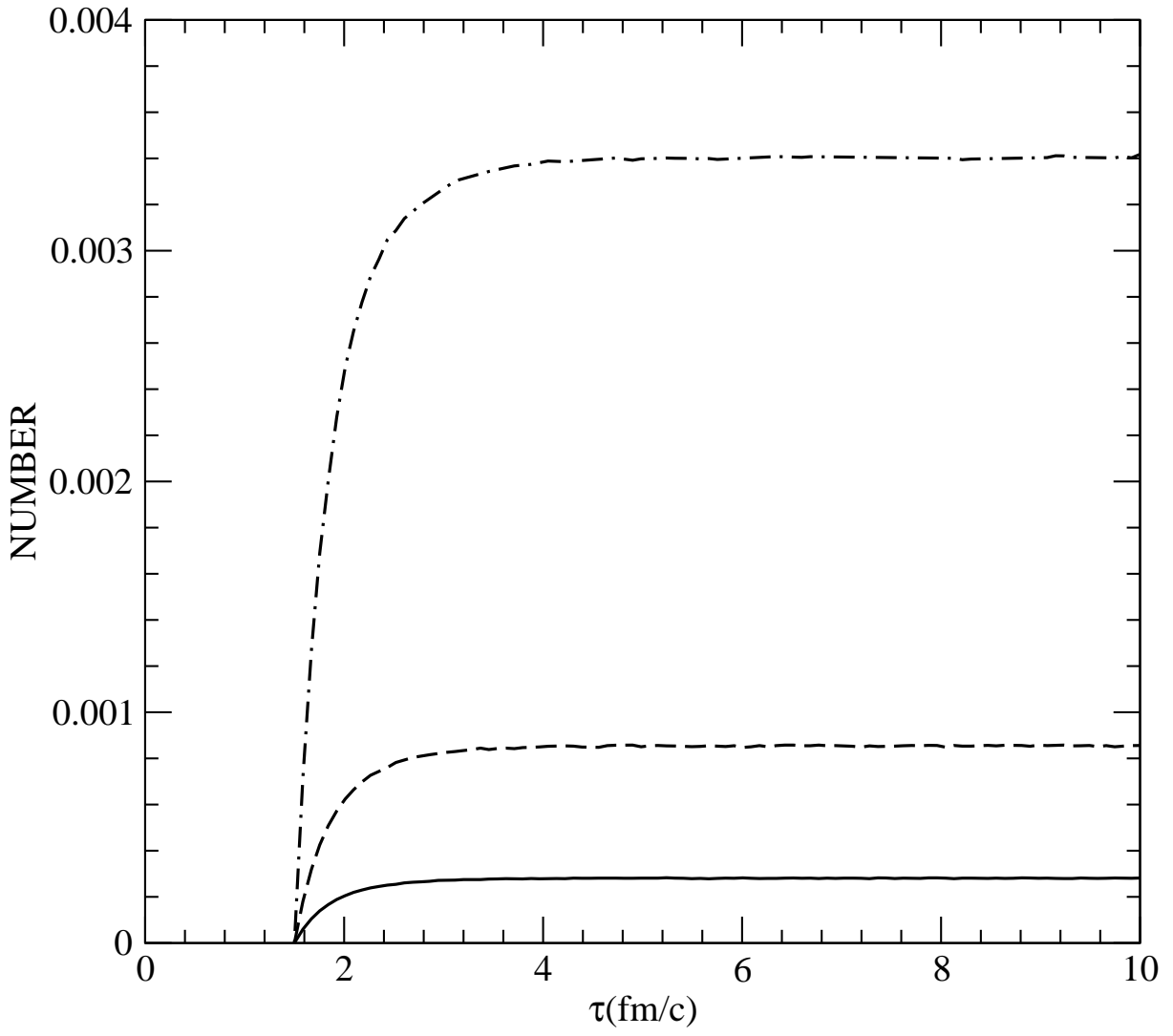


Figure 4: